

Relationship between Pyrite Stability and Arsenic Mobility During Aquifer Storage and Recovery in Southwest Central Florida

GREGG W. JONES* AND
THOMAS PICHLER†

Southwest Florida Water Management District, 2379 Broad Street, Brooksville, Florida 34604

Elevated arsenic concentrations are common in water recovered from aquifer storage and recovery (ASR) systems in west-central Florida that store surface water. Investigations of the Suwannee Limestone of the Upper Floridan aquifer, the storage zone for ASR systems, have shown that arsenic is highest in pyrite in zones of high moldic porosity. Geochemical modeling was employed to examine pyrite stability in limestone during simulated injections of surface water into wells open only to the Suwannee Limestone with known mineralogy and water chemistry. The goal was to determine if aquifer redox conditions could be altered to the degree of pyrite instability. Increasing amounts of injection water were added to native storage-zone water, and resulting reaction paths were plotted on pyrite stability diagrams. Native storage-zone water plotted within the pyrite stability field, indicating that conditions were sufficiently reducing to allow for pyrite stability. Thus, arsenic is immobilized in pyrite, and its groundwater concentration should be low. This was corroborated by analysis of water samples, none of which had arsenic concentrations above $0.036 \mu\text{g/L}$. During simulation, however, as injection/native storage-zone water ratios increased, conditions became less reducing and pyrite became unstable. The result would be release of arsenic from limestone into storage-zone water.

Introduction

Aquifer storage and recovery (ASR) is the storage of water in an aquifer through a well when water is available and recovery of the water from the well when it is needed. An impediment to ASR development in Florida is the leaching of arsenic from the aquifer matrix into stored water. During ASR cycle tests at three facilities in the study area, arsenic concentrations were less than $3 \mu\text{g/L}$ in injection and storage-zone water. However, concentrations frequently exceeded $10 \mu\text{g/L}$ and were as high as $130 \mu\text{g/L}$ in recovered water (1). The cause of elevated arsenic concentrations is likely the interaction of injected surface water and aquifer materials in the storage zone (1–3). Although arsenic can be removed from recovered water during treatment, mobilization of arsenic in the aquifer at concentrations exceeding the $10 \mu\text{g/L}$ drinking water standard is prohibited under federal regulations (4).

* Corresponding author phone: (352)796-7211; e-mail: gregg.jones@swfwmd.state.fl.us.

† Current address: Department of Geology, University of South Florida, Tampa, FL 33620.

The question arises as to whether dissolution of pyrite in limestone could be responsible for elevated arsenic concentrations. Building on the findings of Price and Pichler (2, 3), this investigation evaluated whether injection of surface water into the storage zone would cause pyrite to become unstable. Investigation components included: (a) analysis of water samples over a 30-month period from 19 wells dispersed throughout a groundwater basin to characterize water chemistry of the storage zone, (b) analysis of variability of native storage-zone water chemistry, (c) delineation of a subset of wells with water chemistry representative of water types in west-central Florida, (d) determination of background concentrations of arsenic in native storage-zone water using a method capable of quantifying arsenic at low $\mu\text{g/L}$ concentrations, and (e) geochemical modeling of mixing of waters in the storage zone.

Description of the Study Area. The study area is the 13000 km² Southwest-Central Florida Groundwater Basin (Figure 1). The Upper Floridan aquifer is a vertically continuous sequence of highly permeable carbonate rocks (5) approximately 300 m thick. From uppermost to lowermost, the aquifer consists of the Suwannee Limestone of Oligocene age and the Ocala Limestone and Avon Park Formation of Eocene age. The rocks are hydraulically connected to varying degrees, and solution-enlarged fractures contain large quantities of water. The aquifer is confined above by interbedded carbonates, sands, and clays of the Hawthorn Group and below by limestone and dolostones of the Ocala Limestone that contain gypsum and anhydrite (7). The Suwannee Limestone, the storage zone for ASR systems in the study area, is a wackestone mud to pelletal, foraminiferal grainstone (6–9) that contains clay intermixed with limestone near the formation top (5), and a thin layer of dolostone in the lower third (9). Minor amounts of chert nodules, organics, and pyrite are present.

Upper Floridan Aquifer Flow System and Hydrochemistry. The aquifer is recharged in the eastern portion of the basin. Groundwater in this area has a low total dissolved solids (TDS) content and is dominated by calcium, magnesium, and bicarbonate (10). As water moves westward and deeper, TDS increases and sulfate becomes dominant due to gypsum and anhydrite in the Avon Park Formation. Water moves upward as it approaches the coast and becomes dominated by sodium and chloride as it interacts with seawater (10–12).

Arsenic Mobilization in ASR Systems. Price and Pichler (2, 3) conducted mineralogical and geochemical analyses on over 300 core samples from 19 wells in the study area (Figure 1) that were not affected by ASR operations to determine the location of arsenic in the Suwannee Limestone. Results showed that (a) the mean arsenic concentration was 3.5 mg/kg , but is concentrated in trace minerals, particularly framboidal pyrite, (b) framboidal pyrite can contain arsenic at concentrations exceeding 1000 mg/kg and is most abundant in high porosity zones, and (c) hydrous ferric oxides and phosphorite minerals are not important arsenic sources.

Additional evidence supporting arsenic mobilization from pyrite includes (a) correlation of metals common to pyrite such as molybdenum and vanadium with arsenic and iron in the aquifer matrix, (b) mobilization and correlation of arsenic and iron in recovered waters, and (c) redox conditions conducive to pyrite oxidation (1).

These findings are supported by the work of researchers who have shown that pyrite, arsenopyrite, and/or unspecified sulfide minerals are often the primary source of arsenic in groundwaters (13–18).

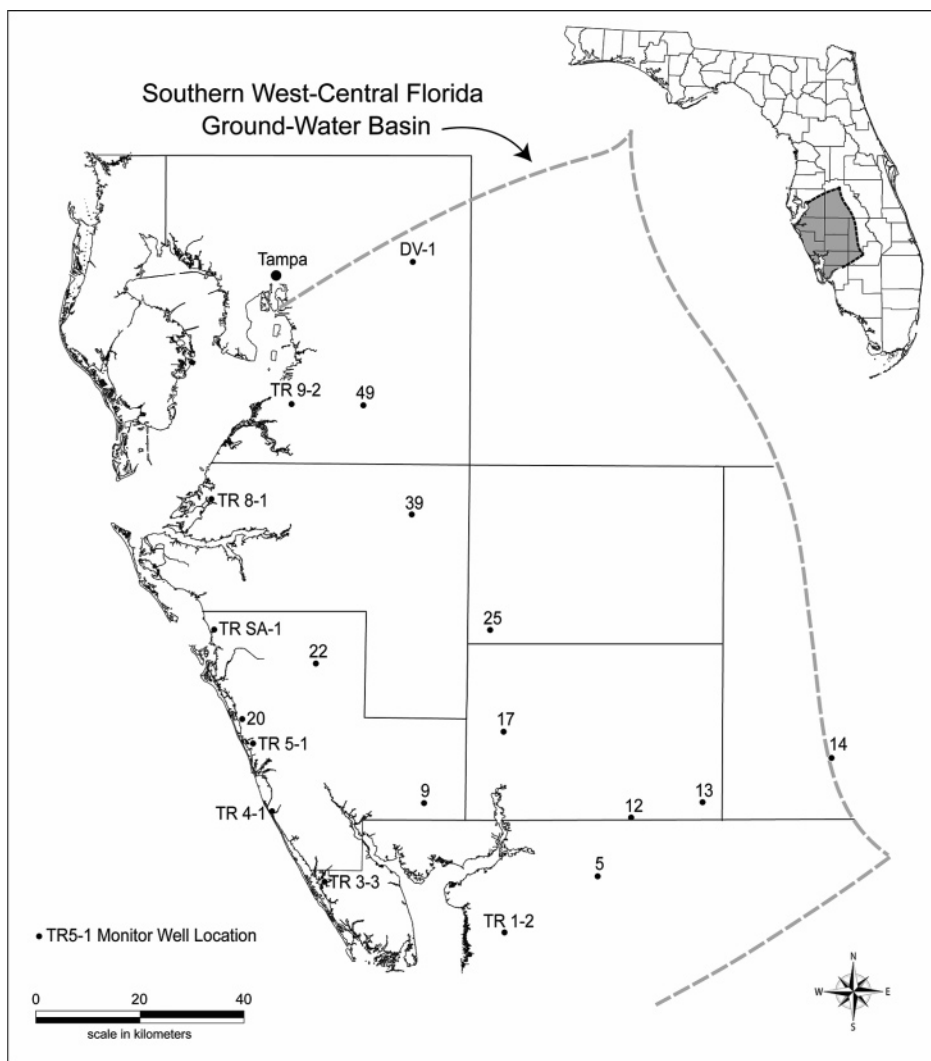


FIGURE 1. Location of the study area and monitor wells.

Methods

Water Chemistry. Waters with different chemistries were used for geochemical modeling of mixing in the storage zone. Native storage-zone water consisted of a recharge end member, a discharge end member (i.e., down-gradient), and an intermediate stage. The chemistry of injection water consisted of the mean of parameters analyzed from numerous samples collected from the City of Tampa's supply system. To characterize native storage-zone water chemistry, samples were collected from 19 wells open to the Suwannee Limestone in May 2002, 2003, and 2004, the end of the dry season, and September 2002 and 2003, the end of the wet season to investigate possible seasonal variations. Field parameters were measured and samples collected in adherence to a quality assurance plan approved by the Florida Department of Environmental Protection. Temperature, dissolved oxygen (DO), conductivity, pH, and Eh were measured within wells using a YSI 600XLM probe. Samples were analyzed for bicarbonate, magnesium, calcium, sodium, potassium, chloride, sulfate, silicon, iron, strontium, and TDS by a state-certified laboratory using standard methodology and QA/QC procedures, that is, EPA Methods 200 and 300. The degree of variability in Eh was unacceptable, and thus the sulfate/sulfide redox couple was used as a redox indicator. Because samples were not analyzed for sulfide for the first four sampling events, in June 2004, additional samples were

collected and analyzed specifically for sulfide in accordance with EPA Method 376.1.

The concentration of arsenic was determined at the University of South Florida's Center for Water Analysis by hydride generation atomic fluorescence spectrometry using a PSA 10.055 Millennium Excalibur system. Samples were consumed with concentrated, ultrapure HCl, and a saturated potassium iodide solution, at a ratio of 68:30:2. This caused reduction of arsenate (As^{5+}) to arsenite (As^{3+}) prior to formation of arsenic hydride (AsH_3) via addition of sodium tetraborohydride ($NaBH_4$) (19). EPA method 200.8 (Trace Elements in Natural Waters by ICP-MS) was not suitable for arsenic analysis because concentrations in native storage-zone water were generally below $1.4 \mu g/L$, the method detection limit. Injection water was obtained from the Hillsborough River and is used in the City of Tampa's ASR system. The water was chloraminated and potentially ozonated prior to injection. Water-chemistry data were obtained from samples collected between January 2001 and May 2003. All analyses were conducted by the City's state certified laboratory.

Geochemical Modeling. Modeling was used to examine pyrite stability as a function of mixing injection and storage-zone waters where the injection/storage-zone water ratio was increased exponentially at each step. The modeling process was as follows.

TABLE 1. Parameter Means for City of Tampa Injection Water and Five Sampling Events for 19 Wells

water source	T ^a	DO ^b	pH	SO ₄ ^b	S ^b	Cl ^b	Ca ^b	Mg ^b	Na ^b	K ^b	SiO ₂ (aq) ^b	Fe ^b	HCO ₃ ^b	Sr ^b	As ^c
City of Tampa injection water	25.8	15.4	7.6	114.0	nd	28.7	88.9	9.5	61.0	1.9	nd	0.10	81.9	nd	nd
monitor wells															
12	27.7	0.28	7.6	138.8	7.3	273.5	75.4	36.8	131.2	4.1	18.7	<0.012	124.4	27.9	<0.02
13	27.0	0.23	7.7	72.0	7.6	96.7	40.8	22.5	58.6	3.1	17.4	<0.012	124.3	15.0	<0.02
14	25.6	0.28	8.7	12.9	3.2	7.4	4.2	4.1	49.4	4.2	10.6	<0.012	115.9	1.4	<0.02
17	27.3	0.31	7.2	363.5	9.1	67.1	108.0	60.6	38.0	4.1	24.4	<0.012	157.8	16.8	<0.02
20	28.2	0.37	6.9	1676.7	5.0	278.7	486.6	175.0	142.8	7.2	22.9	0.05	133.5	15.0	<0.02
22	25.4	0.58	7.2	367.6	9.8	22.3	110.0	56.0	18.2	3.1	25.8	<0.012	161.1	16.7	0.022
25	28.1	0.20	7.2	555.3	8.2	17.1	151.0	70.7	14.3	3.5	26.5	0.06	140.4	21.1	0.029
39	27.1	0.28	7.4	128.8	4.9	13.8	62.2	27.4	10.3	2.1	21.3	<0.012	152.4	5.9	<0.02
49	25.9	0.22	7.5	58.1	1.9	14.1	48.1	20.5	10.7	1.3	24.7	<0.012	156.1	1.9	0.026
5	30.0	0.36	7.4	212.6	6.7	726.7	107.3	75.2	317.8	12.1	18.3	<0.012	98.3	48.6	<0.02
9	27.9	0.54	7.1	342.7	12.0	514.2	136.0	71.9	250.5	8.6	22.7	0.07	156.2	29.1	<0.02
TR 1-2	30.9	0.25	7.3	270.7	11.0	986.5	129.0	103.7	440.2	18.2	17.6	<0.012	122.8	27.9	<0.02
TR 4-1	28.5	0.53	6.9	623.7	8.6	3278.6	496.0	262.4	1382.0	18.7	23.1	0.04	154.9	37.9	0.035
TR 8-1	26.4	0.66	7.3	467.7	6.1	129.2	151.3	66.0	62.7	3.9	23.6	<0.012	144.1	11.8	0.036
TR 9-2	26.8	0.73	7.2	380.3	5.5	213.8	154.0	71.1	65.3	2.3	22.7	<0.012	142.9	6.8	<0.02
TR SA-1	27.8	0.55	7.1	1043.6	6.3	791.1	323.6	142.6	387.4	12.1	23.4	0.05	128.4	21.7	<0.02
DV-1	24.9	0.27	7.3	0.1	2.9	6.0	52.1	9.6	6.3	0.8	30.9	0.40	185.6	0.3	0.022
TR 5-1	26.4	0.32	7.0	1531.0	7.7	100.8	423.4	154.6	55.1	5.3	24.5	0.10	126.8	14.3	<0.02
TR 3-3	28.5	0.34	7.0	1228.0	6.1	8740.4	467.7	543.2	4428.2	139.3	19.7	0.06	153.0	61.8	<0.02

^a °C. ^b mg/L. ^c µg/L.

atmosphere, would prevent significant seasonal variation of the water chemistry within each well. The low degree of variability was verification that, for each well, it was appropriate to use the mean of the five values for each parameter for modeling. Table 1 is a compilation of parameter means for the City of Tampa's water system and for the 19 wells.

Determination of Representative Water Types. Plotting samples on a Piper diagram revealed the pattern of chemical evolution in the flow system originally described by Back and Hanshaw (10). Water enters the aquifer in the eastern portion of the study area, travels to the southwest, and discharges into the Gulf of Mexico. Water analyses from the 19 wells that comprised this pattern can be characterized by wells at three points in the flow system that represent distinct water types: a recharge end member, a discharge end member, and an intermediate stage. The recharge end member, dominated by calcium and bicarbonate, had a low TDS concentration (212 mg/L) and entered the aquifer much more recently relative to the other water types. Well DV-1 was chosen as being most representative of water chemistry in the recharge area. The intermediate stage, dominated by calcium, magnesium, and sulfate, had a higher TDS concentration (2500 mg/L) and had migrated westward and deep into the flow system and interacted with gypsum and anhydrite (26). Well TR 5-1 was most representative of this portion of the flow system. Although this well is located only 2.4 km from the coast, it is inland of the saltwater/freshwater interface and, therefore, does not have the sodium/chloride dominance characteristic of the discharge end member. The discharge end member, dominated by sodium and chloride, had the highest TDS concentration (15877 mg/L). This water was mixing with seawater in the aquifer prior to discharging into the Gulf of Mexico. Well TR 3-3 was most representative of this down-gradient portion of the flow system.

Reaction Paths. The injection of surface water into the three representative wells was simulated. As stated above, data from the City of Tampa's public supply system were used to characterize injection water. Figures 3–5 are a series of stability diagrams of the Fe–S system for wells DV-1, TR 5-1, and TR 3-3, respectively. Each well has six diagrams. Diagram A depicts the mineral stability fields for the Fe–S system in the storage zone in contact with native storage-zone water. The "■" shows where the log activity of the

sulfate/sulfide ratio versus pH of the analyses for unmixed storage-zone water plots. Diagram B is unmixed storage-zone water, but the scale for the y-axis is magnified to focus on the pyrite stability field. The scale remains magnified for diagrams C–F, which depict stability fields of minerals in contact with injection/storage-zone water mixtures with ratios of 1×10^2 to 1, 1×10^5 to 1, 1×10^9 to 1, and 1×10^{15} to 1, respectively. The log activity of the sulfate/sulfide ratio versus pH of storage-zone water and of the corresponding injection/storage-zone water mixture is plotted on each diagram.

pH was not relevant in determining pyrite stability because pH of the storage-zone water, injection water, and mixtures of the two encompassed a narrow range that was within the pH dimension of the pyrite stability field.

The reaction paths for all three wells were fairly similar. Pyrite was stable in contact with the native storage-zone water in all three wells (Figures 3A,B–5A,B). Between injection/storage-zone water mixing ratios of 1×10^2 to 1 and 1×10^5 to 1, the waters plotted higher in the pyrite stability field due to increasing proportions of oxygenated injection water (Figures 3C,D–5C,D). At a mixing ratio of 1×10^9 to 1, the limit of pyrite stability was approached, and, beyond this, pyrite became unstable (Figures 3E,F–5E,F).

Regarding variation in pyrite stability field size, the low sulfate concentration for storage-zone water in DV-1 (0.13 mg/L) (Figure 3B) resulted in a smaller field than that of TR 5-1 (Figure 4B) and TR 3-3 (Figure 5B) with sulfate concentrations of 1531 and 1228 mg/L, respectively. For DV-1, the field increased in size from native storage-zone water to water with a mixing ratio of 1×10^2 to 1 (Figure 3B,C), as low sulfate native storage-zone water was mixed with injection water with a sulfate concentration of 114 mg/L. Between mixing ratios of 1×10^2 to 1 and 1×10^5 to 1, the field size decreased for DV-1 (Figure 3C,D). Although the sulfate concentration had stabilized, the iron concentration declined as native storage-zone water, with an iron concentration of 0.4 mg/L, was mixed with injection water with an iron concentration of 0.1 mg/L. Beyond a mixing ratio of 1×10^5 to 1, field size did not change because sulfate and iron concentrations stabilized (Figure 3E,F).

For TR 5-1 (Figure 4) and TR 3-3 (Figure 5), pyrite stability field size decreased from the native storage-zone water to a

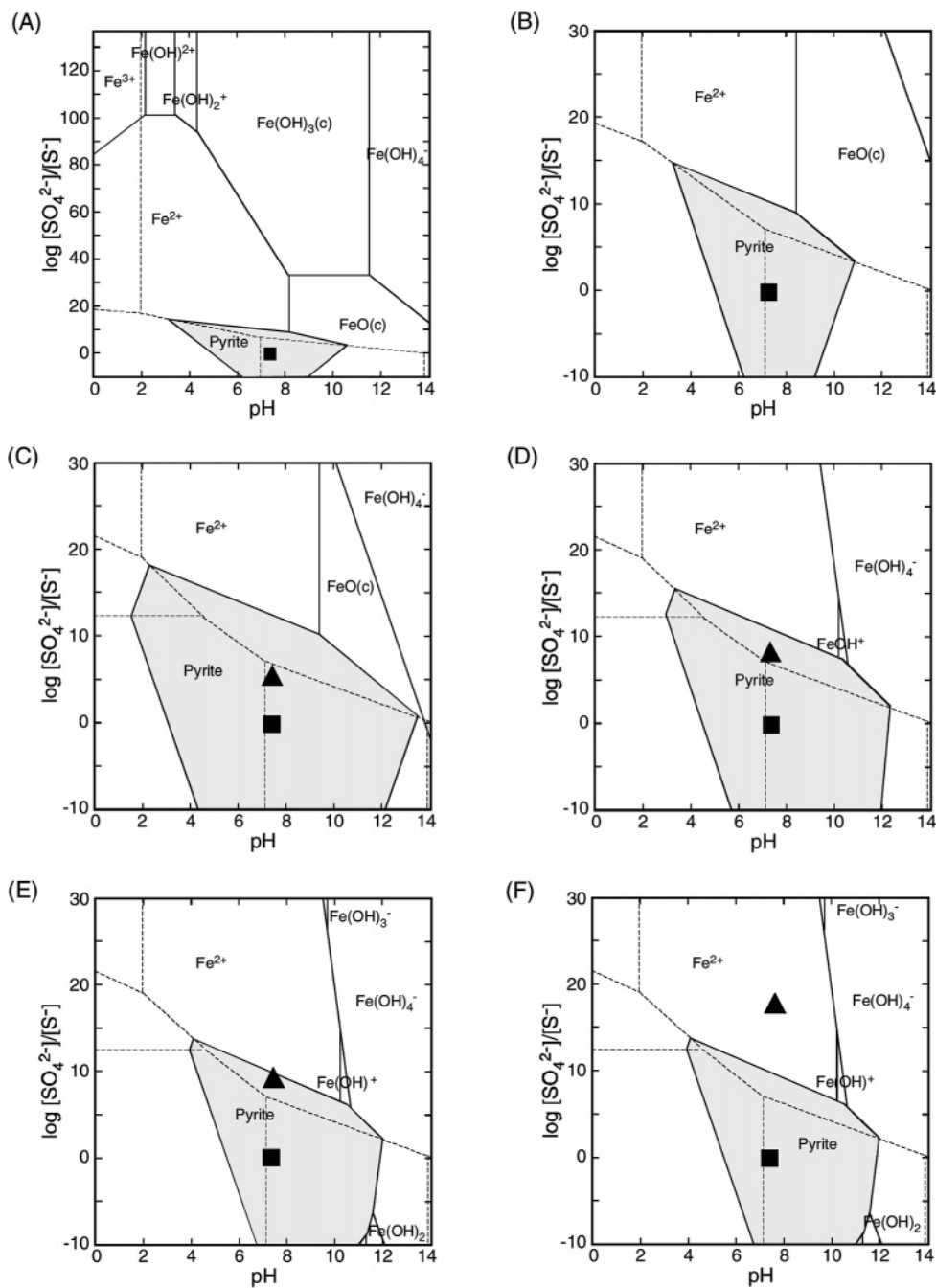


FIGURE 3. Fe–S stability diagrams showing pyrite stability during simulated injection of surface water into DV-1. The native storage-zone water and the mixture of injection/storage-zone water plot as a ■ and ▲, respectively. (A) Native storage-zone water. (B) Magnification of the pyrite stability field in (A). (C), (D), (E), and (F) are injection/storage-zone water mixtures of 1×10^2 to 1, 1×10^5 to 1, 1×10^9 to 1, and 1×10^{15} to 1, respectively.

point at or before the 1×10^9 to 1 mixture because the high sulfate concentration of the native storage-zone waters (1531 and 1228 mg/L, respectively) was diluted by larger volumes of lower sulfate injection water. This also explains why the FeSO_4 field in Figures 4B and 5B changed to Fe^{2+} in Figures 4C and 5C.

Iron did not have a significant impact on pyrite stability field size for these wells because the iron concentrations of injection and TR 5-1 native storage-zone water were equal (0.1 mg/L). Although the iron concentration of TR 3-3 native storage-zone water (0.06 mg/L) was lower than that of injection water (0.1 mg/L), the much greater magnitude of changes in sulfate concentrations as native storage-zone and injection waters were mixed overshadowed the effect of changes in iron concentrations.

Reaction Paths and Arsenic Occurrence. That pyrite in limestone was stable in contact with native storage-zone water for all three wells indicated that redox conditions in the Suwannee Limestone were reducing. As stated previously, arsenic in the Suwannee Limestone is concentrated in framboidal pyrite (1, 2, 27). Because modeling shows that pyrite is stable in limestone in contact with native storage-zone water for all three wells, the arsenic concentration in water in the wells should be very low. This was verified by the analysis of arsenic in samples from the wells, which indicated arsenic concentrations less than or equal to 0.036 $\mu\text{g/L}$ (Table 1).

As the injection/storage-zone water ratio increased, redox conditions became more oxidizing, and the mixtures plotted higher in the pyrite stability field. At injection/storage-zone

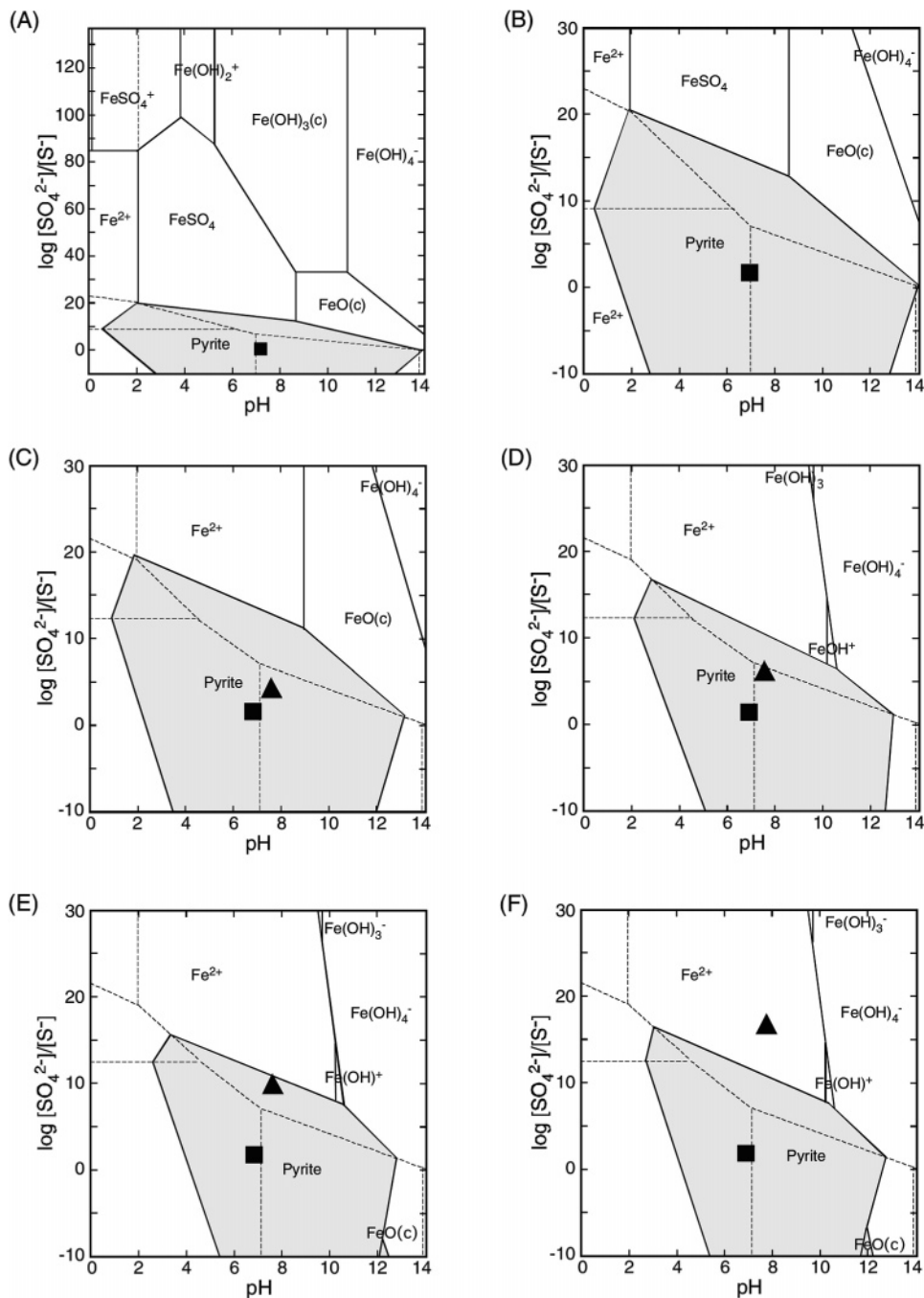


FIGURE 4. Fe–S stability diagrams showing pyrite stability during simulated injection of surface water into TR 5-1. See the caption of Figure 3 for an explanation of each diagram.

water mixing ratios above 1×10^9 to 1, pyrite became unstable and dissolved. The result of dissolution is thought to be the release of arsenic immobilized in pyrite into solution. The reaction for pyrite oxidation is: $\text{FeS}_2 + 3.5/\text{O}_2 + \text{H}_2\text{O} \rightleftharpoons \text{Fe}^{2+} + 2\text{SO}_4^{2-} + 2\text{H}^+$. When this occurs, ferrous iron, sulfate, arsenic, and other trace metals associated with pyrite are released from limestone into storage-zone water (1, 27). While increases in arsenic and ferrous iron have been observed in water recovered from ASR systems, along with a subsequent decrease in DO (26–28), an increase in sulfate is difficult to detect because of high background concentrations.

Hydrous Ferric Oxides and Arsenic Occurrence. Iron can precipitate from solution to form colloidal and suspended oxide, hydroxide, and oxyhydroxide phases known as hydrous ferric oxides (HFOs, $\text{FeOOH} \cdot n\text{H}_2\text{O}$). HFOs are highly soluble

under acidic conditions but nearly insoluble at near-neutral pH (28), and due to their large specific surface areas, they readily adsorb metals from solution (29). Ferrihydroxide, for example, can have arsenic concentrations greater than 5 wt % (30). The mineralogical investigation of the Suwannee Limestone (2) found HFOs in only three core samples out of over 300 analyzed. These occurred as oxidation halos around framboidal pyrite and could have resulted from pyrite oxidation during drilling or core storage. HFOs would not be common in the reducing conditions of the storage zone because they are generally stable only in oxidizing environments (31). This is apparent in Figures 3A–5A where HFO stability fields are in the portion of the diagrams that is significantly more oxidized than the pyrite stability field.

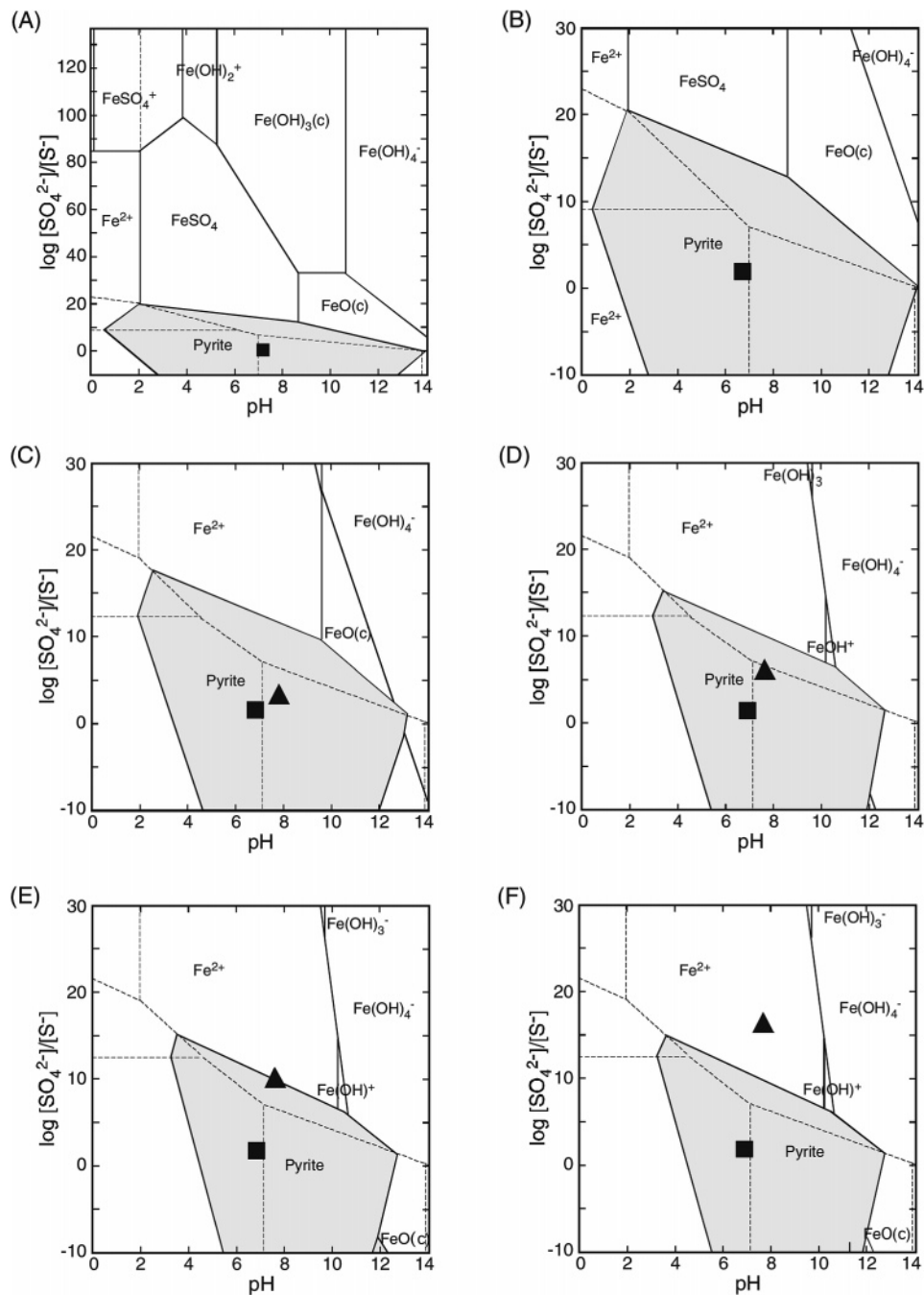


FIGURE 5. Fe–S stability diagrams showing pyrite stability during simulated injection of surface water into TR 3-3. See the caption of Figure 3 for an explanation of each diagram.

It has been suggested that when pyrite is oxidized and arsenic is released, HFOs could sorb arsenic from solution, attenuate the arsenic concentration, and, under the appropriate conditions, dissolve and release arsenic to solution. Figures 3–5 suggest that HFOs are not stable in the full range of waters from native storage-zone water to nearly pure injection water. This indicates that arsenic could not be removed from solution by HFOs as modeled herein.

Microbiological Activity and Pyrite Stability. It is difficult to determine whether microbes have a significant role in pyrite oxidation during surface water injection. We speculate that the role of microbes would not be important in the immediate vicinity of an ASR well. This is because the pyrite oxidation potential of the ozonated and chloraminated injection water as well as its toxicity to microbes would be high when it initially contacts storage-zone limestone. As

the injection water moves further into the storage zone, its potential to oxidize pyrite and its toxicity to microbes would probably diminish rapidly. How rapidly this occurs depends on the injection water's initial concentration of chloramines and degree of ozonation. At some distance from the injection well, the reduced toxicity of the injection water and the presence of nutrients in the injection water could stimulate microbes that would be capable of oxidizing pyrite.

Acknowledgments

This research was funded by the Southwest Florida Water Management District. We thank Roy Price and Olesya Lazareva, University of South Florida, Dr. Jon Arthur, Florida Geological Survey, and the Water Management District for invaluable assistance.

Literature Cited

- (1) Arthur, J. D.; Dabous, A. A.; Cowart, J. B. Water-Rock Geochemical Consideration for Aquifer Storage and Recovery: Florida Case Studies. In *Underground Injection Science and Technology, Developments in Water Science*; Tsang, C. F., Apps, J. A., Eds.; Elsevier: Amsterdam, 2005; Vol. 52, pp 327–339.
- (2) Price, R. E.; Pichler, T. Oxidation of Framboidal Pyrite as a Mobilization Mechanism During Aquifer Storage and Recovery in the Upper Floridan Aquifer, Southwest Florida. *EOS Trans., Am. Geophys. Union* **2002**, *83*, 47.
- (3) Price, R. E.; Pichler, T. Abundance and Mineralogic Association of Arsenic in the Suwannee Limestone (Florida): Implications for Arsenic Release During Water-Rock Interaction. *Chem. Geol.* **2005**, *228*, 44–56.
- (4) Code of Federal Regulations, Title 40, Part 144, Underground Injection Control Program.
- (5) Miller, J. A. Hydrogeologic Framework of the Floridan Aquifer System in Florida and in Parts of Georgia, Alabama, and South Carolina; U.S. Geological Survey Professional Paper 1403-B; 1986.
- (6) Gilboy, A. E. Hydrogeology of the Southwest Florida Water Management District; Southwest Florida Water Management District Technical Report 85-01; Brooksville, FL, 1985.
- (7) Hammes, U. Sedimentation Patterns, Sequence Stratigraphy, Cyclicity, and Diagenesis of Early Oligocene Carbonate Ramp Deposits, Suwannee Formation, Southwest Florida; Ph.D. Thesis, University of Colorado, Boulder, CO, 1992.
- (8) Williams, H.; Cowart, J. B.; Arthur, J. D. Florida ASR Geochemical Study, S.W. Florida: Year One and Two Progress Report. Florida Geological Survey, Tallahassee, FL, 2002.
- (9) Green, R.; Arthur, J. D.; DeWitt, D. Lithostratigraphic and Hydrostratigraphic Cross Sections through Pinellas and Hillsborough Counties, Southwest Florida. Florida Geological Survey Open File Report 61; 1995.
- (10) Back, W.; Hanshaw, B. B. Comparison of Chemical Hydrogeology of the Carbonate Peninsulas of Florida and Yucatan. *J. Hydrol.* **1970**, *10*, 330–368.
- (11) Plummer, L. N. Defining Reactions and Mass Transfer in Part of the Floridan Aquifer. *Water Resour. Res.* **1977**, *13*, 801–812.
- (12) Plummer, L. N.; Parkhurst, D. L.; Thorsteson, D. C. Development of Reaction Models for Groundwater Systems. *Geochim. Cosmochim. Acta* **1983**, *47*, 665–685.
- (13) Gotkowitz, M. B.; Schreiber, M. E.; Simo, T. Delineating Causes of Arsenic Contamination of Groundwater, Eastern Wisconsin. *EOS Trans., Am. Geophys. Union Fall Meeting Suppl.* **2000**, *81*, 52.
- (14) Nickson, R. T.; McArthur, J. M.; Ravenscroft, P.; Burgess, W. G.; Ahmed, K. M. Mechanism of Arsenic Release to Groundwater, Bangladesh and West Bengal. *Appl. Geochem.* **2000**, *15*, 403–413.
- (15) Peters, S. C.; Blum, J. D.; Klaue, B.; Karagas, M. R. Arsenic Occurrence in New Hampshire Drinking Water. *Environ. Sci. Technol.* **1999**, *33*, 1328–1333.
- (16) Robinson, G. R.; Ayotte, J. D.; Ayuso, R. A. Arsenic in Bedrock, Groundwater, and Soils in New England. *EOS Trans., Am. Geophys. Union Fall Meeting Suppl.* **2000**, *81*, 524.
- (17) Serfes, M. E.; Spayd, S. E.; Herman, G. C.; Montverde, D. E. Arsenic Occurrence, Source, and Possible Mobilization Mechanisms in Groundwater in the Piedmont Physiographic Province in New Jersey. *EOS Trans., Am. Geophys. Union Fall Meeting Suppl.* **2000**, *81*, 525.
- (18) Smedley, P. L.; Kinniburgh, D. G. A Review of the Source and Behavior and Distribution of Arsenic in Natural Waters. U.N. Synthesis Report on Arsenic in Drinking Water; World Health Organization: Geneva, 2001.
- (19) Price, R. E.; Pichler, T. Distribution, Speciation and Bioavailability of Arsenic in a Shallow-Water Submarine Hydrothermal System, Tutum Bay, Ambitle Island, PNG. *Chem. Geol.* **2005**, *224*, 122–135.
- (20) Piper, A. M. A Graphic Procedure in the Geochemical Interpretation of Water Analyses. *Am. Geophys. Union Trans.* **1944**, *25*, 914–923.
- (21) Stumm, W.; Morgan, J. J. *Aquatic Chemistry, An Introduction Emphasizing Chemical Equilibria in Natural Waters*, 2nd ed.; John Wiley and Sons: New York, 1981.
- (22) Hostettler, J. D. Electrode Potentials, Aqueous Electrons, and Redox Potentials in Natural Water. *Am. J. Sci.* **1984**, *284*, 734–759.
- (23) Lindburg, R. D.; Runnels, D. D. Groundwater Redox Reactions: an Analysis of Equilibrium State Applied to Eh Measurements and Geochemical Modeling. *Science* **1984**, *225*, 925–927.
- (24) Runnels, D. D.; Lindburg, R. D. Selenium in Aqueous Solutions: the Impossibility of Obtaining a Meaningful Eh Using a Platinum Electrode, with Implications for Modeling of Natural Waters. *Geology* **1990**, *18*, 212–215.
- (25) Hanshaw, B. B.; Back, W.; Rubin, M. Carbonate Equilibria and Radiocarbon Distribution Related to Groundwater Flow in the Floridan Limestone Aquifer, U.S.A. *Science* **1965**, *148*, 494–495.
- (26) Sacks, L. A.; Tihansky, A. B. Geochemical and Isotopic Composition of Groundwater, with Emphasis on Sources of Sulfate, in the Upper Floridan Aquifer and Intermediate Aquifer System in Southwest Florida. U.S. Geological Survey Water Resource Investigations Report 96-4146; 1996.
- (27) Arthur, J. D.; Dabous, A. A.; Cowart, J. B. Mobilization of Arsenic and Other Trace Elements During Aquifer Storage and Recovery, Southwest Florida. Florida Geological Survey Open File Report 02-89; 2002; pp 44–47.
- (28) Mericki, J. E. Water Quality Changes During Cycle Tests at Aquifer Storage Recovery (ASR) Systems of South Florida. ERDC Technical Report 2002, U.S. Army Engineer Research and Development Center, Vicksburg, MS.
- (29) Bethke, C. M. *Geochemical Reaction Modeling*; Oxford University Press: New York, 1996.
- (30) Dzombak, D. A.; Morel, F. M. M. *Surface Complexation Modeling*; John Wiley and Sons: New York, 1990.
- (31) Pichler, T.; Veizer, J.; Hall, G. E. M. Natural Input of Arsenic into a Coral-Reef Ecosystem by Hydrothermal Fluids and its Removal by Fe(III) Oxyhydroxides. *Environ. Sci. Technol.* **1999**, *33*, 1373–1378.

Received for review August 8, 2006. Revised manuscript received October 9, 2006. Accepted October 10, 2006.

ES061901W